ADVANCED OPTICAL MATERIALS

Supporting Information

for *Adv. Optical Mater.,* DOI: 10.1002/adom.202102723

Altering the Reflection Phase for Nano-Polaritons: A Case Study of Hyperbolic Surface Polaritons in Hexagonal Boron Nitride

Mingyuan Chen, Stephen Sanders, Jialiang Shen, Jiahan Li, Eli Harris, Cheng-Chien Chen, Qiong Ma, James H. Edgar, Alejandro Manjavacas, and Siyuan Dai**

Supporting Information

Altering the reflection phase for nano-polaritons: a case study of hyperbolic surface polaritons in hexagonal boron nitride

Mingyuan Chen[||], *Stephen Sanders*[||], *Jialiang Shen, Jiahan Li, Cheng-Chien Chen, Qiong Ma, James Edgar, Alejandro Manjavacas*, Siyuan Dai**

1. Finite element method (FEM) simulation of HSPs in hBN

The numerical analysis of the propagation and reflection of HSPs along the edge and corners of the hBN microstructures was performed by rigorously solving Maxwell's equations using a finite element method (FEM) approach implemented in the commercial software COMSOL Multiphysics. The geometry consisted of a three-dimensional wedge carved out of a hBN slab with a thickness of 22 nm, located on top of an infinitely thick SiO_2 substrate. The dielectric function of hBN and SiO_2 were taken from tabulated data[1, 2]. The wedge was formed by two straight edges of identical length L_0 = 4 μm connected at an angle that was varied from 90º to 300º. We placed two numerical waveguide ports (Port 1 and Port 2) at the ends of the straight edges, as shown in Figures 2b and 2c (notice that, in these panels, we use L_0 = 2 μm to improve visibility, however, all of the numerical results presented here and in the main text were obtained from a model with L_0 = 4 μm). Port 1 was configured to excite the fundamental branch of HSPs [3] at the IR frequency ω = 1419 cm^{-1}. As shown in **Figure S1**, the mode profile shows that the corresponding electric field is mainly confined at the edge of the hBN microstructure, which confirmed that the launched waves were indeed HSPs. Upon solving the model, we calculated the spatial distribution of the vertical component of the electric field 70 nm above the top surface of the hBN microstructure, from which we extracted the line cuts shown in Figure 2d. All of the calculations were checked for convergence with respect to mesh and domain size.

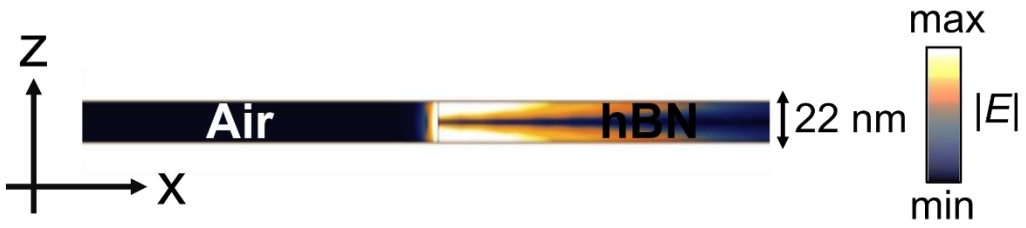

Figure S1. Simulated electric field profile of the HSP modes in hBN. The plot was extracted from the vertical cut plane of the hBN sidewall in the simulation. The thickness of the hBN in the simulation model is 22 nm, and the frequency is $\omega = 1419\ cm^{-1}$.

2. Extraction and normalization of the $|E_z|$ line profiles from the FEM simulation

In order to analyze the electric field profiles on the edge of the hBN microstructures, we extracted $|E_z|$ along a line parallel to the edge of, but 70 nm above, the hBN microstructure. The results are plotted in **Figure S2**a as a function of the distance to the corner L. In order to compare with the s-SNOM data, we removed the overall exponential decay by normalizing the line profiles to that of $\alpha = 180^o$. As shown in Figure S2b, all line profiles from different corner angles show similar results to the s-SNOM line profiles as mentioned in the main text.

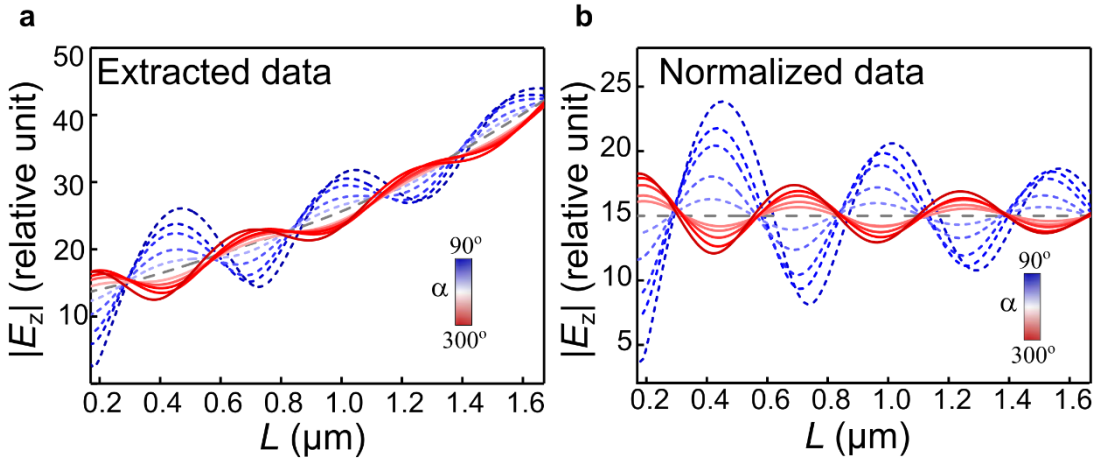

Figure S2. Extracted $|E_z|$ line profiles of HSPs in hBN for different corner angles. a) Directly extracted $|E_z|$ line profile from the FEM simulation. b) Normalized $|E_z|$ line profiles. The gray dashed line represents the data for $\alpha = 180^o$.

3. Extraction of the reflection coefficient from the FEM simulation

As mentioned in the main text, the $|E_z|$ line profiles can be fitted to an analytical model based on the superposition of two counterpropagating plane waves: one describing the HSPs

launched at the port and the other representing their reflection from the corner. Using this model, we can write the amplitude of the vertical component of the electric field of the HSPs at a distance L from the corner as:

$$|E_z(L)| = |E_0 e^{ik_p(L_0-L)} + E_0 r e^{i\phi} e^{ik_p L_0} e^{ik_p L}|, \quad \text{(S1)}$$

where E_0 is the electric field of HSPs launched at Port 1, $k_p = k_p' + ik_p''$ is the wavevector of the HSPs along the propagation direction (the prime and double primes denote the real and imaginary part, respectively), and L_0 is the distance from Port 1 to the corner. To accurately determine the value of k_p, we first analyzed the FEM simulation results of $\alpha = 180^\circ$. For this corner angle, the reflection amplitude should vanish (i.e., $r = 0$), and hence

$$|E_z(L)| = E_0 e^{-k_p''(L_0-L)} \quad \text{(S2)}$$

Furthermore, we can also write the expression for the real part of E_z

$$\mathrm{Re}\{E_z(L)\} = E_0 e^{-k_p''(L_0-L)} \cos[k_p'(L_0 - L) - \delta] \quad \text{(S3)}$$

as well as for the imaginary part

$$\mathrm{Im}\{E_z(L)\} = E_0 e^{-k_p''(L_0-L)} \sin[k_p'(L_0 - L) - \delta] \quad \text{(S4)}$$

where δ is a constant phase. Therefore, as shown in **Figure S3**, by fitting the results from the FEM simulations to the above equations, and calculating their average, we obtain the following result: $k_p' = 5.644\ \mu m^{-1}$ and $k_p'' = 0.736\ \mu m^{-1}$.

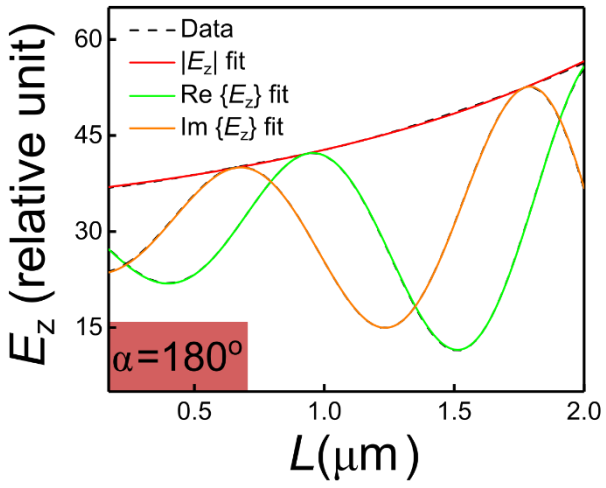

Figure S3. Fitting of the line profile of HSPs for $\alpha = 180^\circ$. Black dashed lines are the FEM simulation data, while the red, green, and orange curves represent the results of the fitting for the absolute, real, and imaginary values of E_z, respectively.

After determining the value of k_p, we can use it to fit all of the remaining simulated $|E_z|$ line profiles for other corner angles (**Figure S4**) to the analytical model and thereby extract the reflection coefficient amplitude r and phase ϕ. As Figure S4 shows, the fits to the analytical model agree very well with the FEM simulation results.

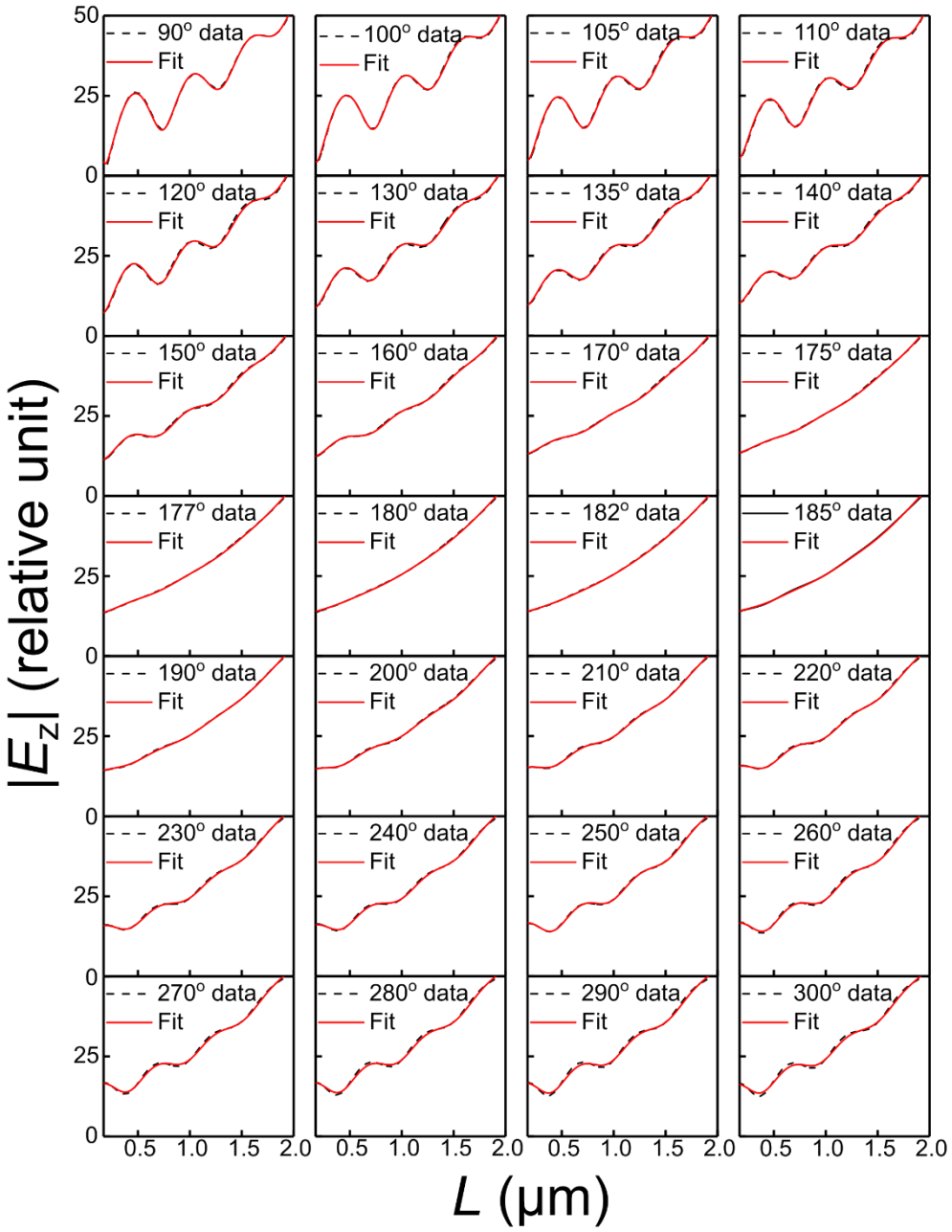

Figure S4. Results of the $|E_z|$ line profile fitting for different corner angles. The dashed black lines represent the data from the FEM simulations, and the red curves are the results of the fitting to the analytical model.

4. Additional FEM simulation of HSPs in hBN

We have performed additional FEM simulations of hBN microstructures with different corner angles α (**Figure S5**), thicknesses *d*, and frequencies ω (**Figure S6**). In addition to the evolution of reflection amplitude *r* and phase ϕ reported in the main text for corner angles in the interval α = 90º – 300º, the results shown in Figure S5a reveal that *r* displays a peak at α ~ 90º, while for α > 300º it seems to saturate. At the same time, Figure S5b shows that ϕ follows the evolution trend reported in the main text. Specifically, for α < 90º, it decreases with decreasing α, and for α > 300º, it increases with increasing α. Furthermore, as shown in Figure S6, the evolution of the reflection phase ϕ as a function of the corner angle α seems to be largely independent of the hBN thickness *d* and the frequency ω. This is consistent with the fact that the polaritonic phenomena in these various specimens are all governed by the mathematical properties of the complex reflection coefficient discussed in Figure 3c.

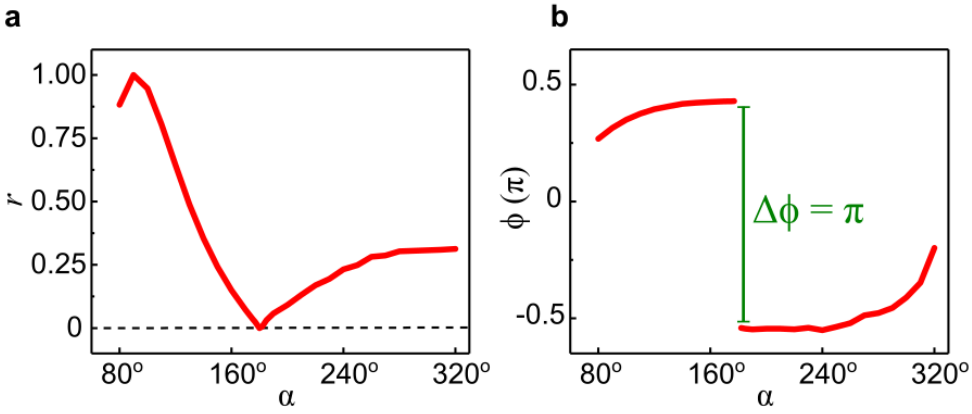

Figure S5. Evolution of the polariton reflection amplitude *r* and phase ϕ as a function of the hBN microstructure corner angle α. We assume a hBN thickness *d* = 22nm and a frequency ω = 1419 cm^{-1}.

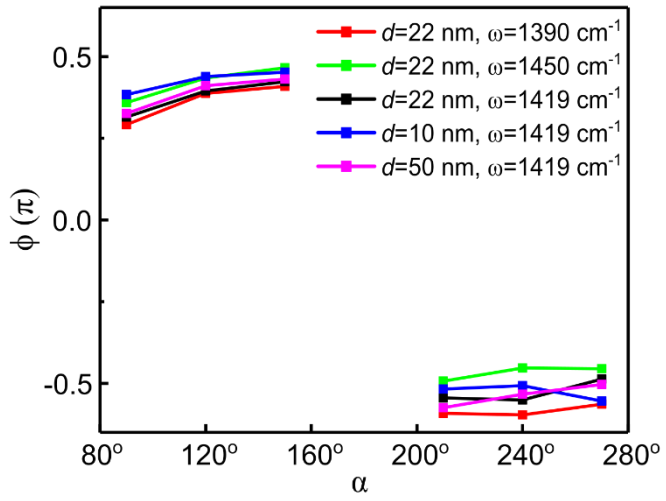

Figure S6. Evolution of the polariton reflection phase ϕ as a function of the hBN microstructure corner angle α for various thicknesses *d* and frequencies ω.

References

[1] J. D. Caldwell, A. V. Kretinin, Y. Chen, V. Giannini, M. M. Fogler, Y. Francescato, C. T. Ellis, J. G. Tischler, C. R. Woods, A. J. Giles, M. Hong, K. Watanabe, T. Taniguchi, S. A. Maier, K. S. Novoselov, *Nat. Commun.* **2014**, *5*, 5221.
[2] A. Kučírková, K. J. A. s. Navrátil, *Appl. Spectrosc.* **1994**, *48*, 113.
[3] S. Dai, M. Tymchenko, Y. Yang, Q. Ma, M. Pita-Vidal, K. Watanabe, T. Taniguchi, P. Jarillo-Herrero, M. M. Fogler, A. Alu, D. N. Basov, *Adv. Mater.* **2018**, *30*, e1706358.